2016 IEEE/RSJ International Conference on Intelligent Robots and Systems (IROS)
Daejeon Convention Center
October 9-14, 2016, Daejeon, Korea

Analytical Investigation of the Stabilizing Function of the Musculoskeletal System using Lyapunov Stability Criteria and its Robotic Applications

Handdeut Chang[1], Sangjoon J. Kim[1], and Jung Kim[1*], *Member, IEEE*

Abstract— **The stabilization of man-made artificial systems has been achieved by sensor based state feedback control with high computational bandwidth and high stiffness structures. In contrast, many biological systems have been achieved similar or superior stable behavior with low speed signal transmission via nervous systems, which is easy to introduce unstable performance from a control engineering perspective. In order to explain this phenomenon, the concept of self-stabilization has recently been proposed and investigated. Self-stabilization is defined as the ability to restore its original state after a disturbance without any feedback control. In this paper, the self-stabilizing function of a musculoskeletal system for arbitrary motion in the vertical plane is analytically investigated using Lyapunov stability theory. Based on this investigation we propose a design method to realize the self-stabilizing function of a musculoskeletal system, and experimentally verify that the self-stabilizing function can be physically realized by the proposed Lyapunov function.**

I. Introduction

In classical control theory, feedback control has been widely utilized to improve the stability of systems. Sensors with high resolution and computing power of high bandwidth have been required to achieve stable feedback control of a robot.

In case of human, sensory feedback also plays a significant role in realizing stable movements. However, the sensory system of human has relatively low resolution, computing power, and nerve transmission delay [1, 2] which can cause serious instability problem in engineering systems. To explain the stable human movement, Kawato [3] have instead emphasized the importance of feedforward control and internal inverse dynamics model acquired by feedback learning and stored in cerebellum. In another previous study, Bizzi [4] observed that disturbed arm movement of deafferented monkeys returned to the original target state. The results suggest that stable motion can be obtained by feedforward control and depends on not solely the central nervous system but also the dynamic properties of the musculoskeletal system.

For these reasons, stabilizing function of the musculoskeletal system has been analytically investigated and defined as self-stabilizing function of musculoskeletal system. Wagner [5, 6] analytically derived the self-stabilizing criteria for a single joint of human musculoskeletal system using eigenvalue analysis. Although this result is significant, the condition does not sufficiently explain why the musculoskeletal system can be self-stabilized because the derived self-stabilization criteria using eigenvalue analysis is effective for only static musculoskeletal systems (time-invariant system), not dynamic musculoskeletal systems (time-varying system). To explain the stabilizing function of dynamic musculoskeletal systems, Sugimoto [7] analytically derived new stability criteria for the cyclic motion of a one degree-of-freedom (DoF) musculoskeletal system. However, it should be also theoretically extended to new stability criteria for arbitrary motion of a multi-DoF musculoskeletal system because a one-DoF musculoskeletal model cannot reflect the interference effect among perturbed joints.

In the field of robotics, Plooij [9, 10] attempted to produce a stable feedforward controlled manipulator designed by optimization method in control engineering. The results are

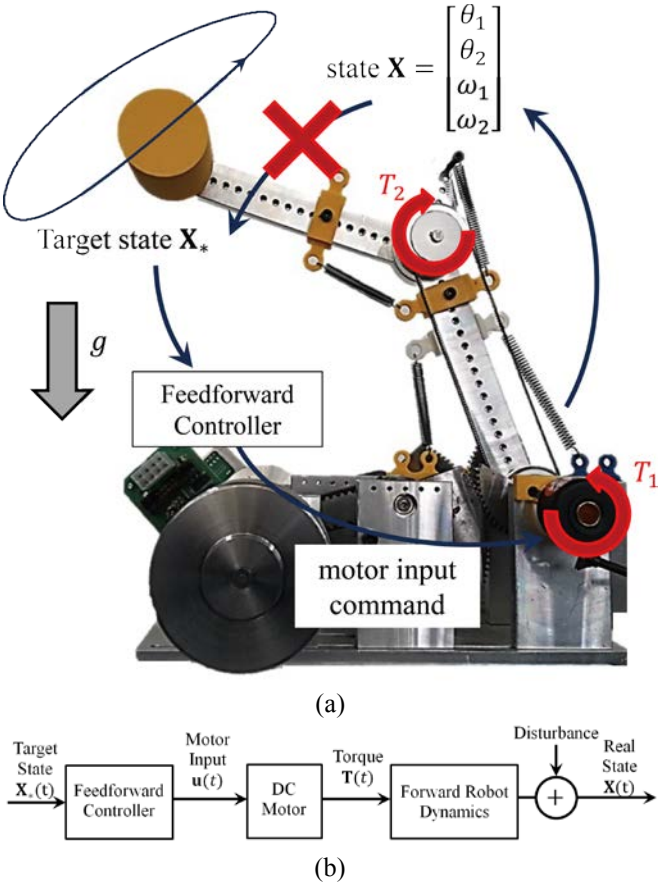

Fig. 1 Designed self-stabilized manipulator (a) and its block diagram (b). The previously determined control input is solely used.

This work was supported by the National Research Foundation of Korea (NRF) grant funded by the Korea government (MSIP) (No. 2015-002966).

Handdeut Chang, Sangjoon J. Kim, Jung Kim are with Korea Advanced Institute of Science and Technology, Daejeon, Korea. (E-mail: onemean, sangjoon.j.kim, and jungkim@kasit.ac.kr).

interesting, but limited because it cannot perform arbitrary motion but only pre-defined specific one cyclic motion.

In this study, we believe that the self-stabilizing function of the biological musculoskeletal system is considered to produce a manipulator that can achieve stabilization of arbitrary motion via a feedforward controller. In our previous study [8], a sufficient condition for the self-stabilization of a two-DoF dynamic musculoskeletal system for arbitrary motion was analytically derived by Lyapunov stability theory which is often used to prove the stability of time-varying systems. In this paper, we will show that biological human musculoskeletal system satisfies the sufficient condition for the self-stabilization and a self-stabilized manipulator can be physically realized (see **Fig. 1**) in both numerical simulation and real world. The self-stabilized manipulator in this paper does not use any sensor for state feedback control but uses only its own body dynamics. These results are significant because they support the hypothesis that stable human motion does not only depend on feedback control of central nervous system but also the dynamics of musculoskeletal system and concept of self-stabilizing function of musculoskeletal system can be applied to robotics field.

II. Stability Analysis of the Musculoskeletal System

A. Mathematical Model of Error System

Fig. 2 shows the model of a two-DoF musculoskeletal system whose joint torque is generated by agonistic and antagonistic muscles. The joint angle coordinate system of **Fig. 2** shows two coordinates: joint angles θ_1 and θ_2. For the upper limb, θ_1 and θ_2 represent the shoulder and elbow joint, respectively. The equation of motion can be expressed in the form of Lagrange's equation.

$$\mathbf{M}\ddot{\boldsymbol{\Theta}} + \mathbf{C}(\boldsymbol{\Theta}) + \mathbf{D}\left(\boldsymbol{\Theta}, \dot{\boldsymbol{\Theta}}\right) = \mathbf{T} \tag{1}$$

where $\mathbf{M}$ is the inertial matrix, $\mathbf{C}$ is the vector for the gravitational force effect, $\mathbf{D}$ is the vector for Coriolis and the centrifugal force effect, $\boldsymbol{\Theta}$ is the joint angle vector, and $\mathbf{T}$ is the joint torque vector. Because the inertial matrix $\mathbf{M}$ is non-singular, the inverse matrix $\mathbf{G} = \mathbf{M}^{-1}$ always exists and satisfies the following equation:

$$\mathbf{G} = \begin{bmatrix} G_{11} & G_{12} \\ G_{21} & G_{22} \end{bmatrix}, \qquad \gamma = \min_t \left[\frac{G_{11}G_{22}}{G_{12}G_{21}}\right] = 1.30$$

$$\frac{G_{11}G_{22}}{G_{12}G_{21}} \simeq \frac{\left(1+\frac{m_2}{4M}\right)\left((1-\cos\theta_2)\left(2+\frac{m_2}{4M}\right)+\frac{m_1}{4M}\right)}{\left((1-\cos\theta_2)\left(1+\frac{m_2}{4M}\right)\right)^2} \tag{2}$$

The value of γ depends on the geometric and mass distribution properties of the musculoskeletal system. In case of a human arm, γ is approximately 1.30. By multiplying both sides of (2) by matrix $\mathbf{G}$, it can be rewritten as follows:

$$\ddot{\boldsymbol{\Theta}} = \mathbf{GT} + \mathbf{H} \tag{3}$$

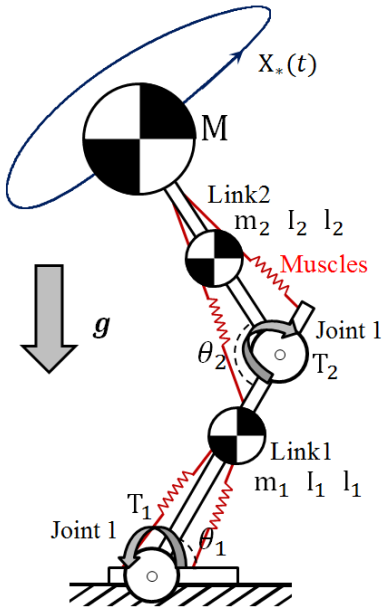

Fig. 2 Two-DoF musculoskeletal model on the vertical plane and its joint angle coordinate system (θ_1 and θ_2). The three point masses (M, m_1, and m_2) and moment of inertias (I_1 and I_2) are modeled.

where $\mathbf{H} = -\mathbf{G}(\mathbf{C} + \mathbf{D})$. For simplification, the equation of motion can be rewritten in the following state equation form:

$$\dot{\mathbf{X}} = \mathbf{F}(\mathbf{X})$$
$$\mathbf{X} = \begin{bmatrix} \theta_1 \\ \theta_2 \\ \omega_1 \\ \omega_2 \end{bmatrix}, \mathbf{F}(\mathbf{X}) = \begin{bmatrix} \omega_1 \\ \omega_2 \\ G_{11}T_1 + G_{12}T_2 + H_1 \\ G_{21}T_1 + G_{22}T_2 + H_2 \end{bmatrix} \tag{4}$$

Then, error system $\mathbf{Z}(t)$ is defined as follows:

$$\mathbf{Z}(t) := \mathbf{X}(t) - \mathbf{X}_*(t) = [Z_{\theta_1} \quad Z_{\theta_2} \quad Z_{\omega_1} \quad Z_{\omega_2}]^T \tag{5}$$

where $\mathbf{X}_*(t)$ is the previously determined target state, and $\mathbf{X}(t)$ is the perturbed real (actual) state. The linear differential equation of the error system $\mathbf{Z}(t)$ is obtained by differentiating (5) with respect to time t and linearizing by Taylor expansion as follows:

$$\begin{aligned} \dot{\mathbf{Z}}(t) &= \dot{\mathbf{X}}(t) - \dot{\mathbf{X}}_*(t) = \mathbf{F}(\mathbf{X}) - \mathbf{F}(\mathbf{X}_*) \\ &= \mathbf{F}(\mathbf{X}_* + \mathbf{Z}) - \mathbf{F}(\mathbf{X}_*) = \frac{\partial \mathbf{F}}{\partial \mathbf{X}}|_{\mathbf{X}=\mathbf{X}_*}\mathbf{Z}(t) + o(||\mathbf{Z}(t)||) \\ \dot{\mathbf{Z}}(t) &\simeq \mathbf{A}(t)\mathbf{Z}(t) \end{aligned} \tag{6}$$

The origin of the error system is the equilibrium point (i.e., $\dot{\mathbf{Z}}(t) = \mathbf{0}$ where $\mathbf{Z} = \mathbf{0}$). Therefore, target state $\mathbf{X}_*(t)$ can also be considered the equilibrium point. The coefficient matrix $\mathbf{A}(t)$ is called the Jacobian matrix and is solely determined by target state $\mathbf{X}_*(t)$ and the behavior of the error system $\mathbf{Z}(t)$ is dominated by this Jacobian matrix. The details of each element in Jacobian matrix $\mathbf{A}(t)$ can be derived as follows:

$$\mathbf{A}(t)=\begin{bmatrix} 0 & 0 & 1 & 0 \\ 0 & 0 & 0 & 1 \\ a_{11}(t) & a_{12}(t) & b_{11}(t) & b_{12}(t) \\ a_{21}(t) & a_{22}(t) & b_{21}(t) & b_{22}(t) \end{bmatrix} \tag{7}$$

$$a_{ii}=G_{ii}\frac{\partial T_i}{\partial \theta_i}+\frac{\partial H_i}{\partial \theta_i}, \qquad a_{ij}=G_{ij}\frac{\partial T_j}{\partial \theta_j}+\frac{\partial H_i}{\partial \theta_j}$$
$$b_{ii}=G_{ii}\frac{\partial T_i}{\partial \omega_i}+\frac{\partial H_i}{\partial \omega_i}, \qquad b_{ij}=G_{ij}\frac{\partial T_j}{\partial \omega_j}+\frac{\partial H_i}{\partial \omega_j}$$

If the origin of the error system (i.e., $\mathbf{Z}=\mathbf{0}$) is a stable equilibrium point, then the musculoskeletal system can be considered to have a self-stabilizing function. It is well known that a system is asymptotically stable if and only if every eigenvalue of a time invariant matrix **A** has a strictly negative real part. However, if the musculoskeletal system dynamically changes its target state, then the error system becomes a time-varying system or a non-autonomous system (i.e., $\mathbf{A}(t)\neq \text{const.}$) and the stability of the origin of (6) is not guaranteed by the negative eigenvalues of $\mathbf{A}(t)$.

As a sufficient condition for the stability of a time-varying system (6), in this study, Lyapunov stability theory is used to investigate the self-stabilizing function of the musculoskeletal system.

B. Sufficient Condition for Self-stabilization

Lyapunov stability theory states that a system is asymptotically stable if a decrescent and positive definite scalar function $V(\mathbf{Z},t):\mathbf{R}^4\times\mathbf{R}_+\rightarrow\mathbf{R}$ exists such that $-\dot{V}(\mathbf{Z},t)$ is also a positive definite scalar function, where t is time, and $\mathbf{Z}$ is the state of the system [11]. $V(\mathbf{Z},t)$ is called a Lyapunov candidate function and the existence of Lyapunov functions is a sufficient condition for system stability. In this study, the following decrescent and positive definite function is defined as a Lyapunov candidate function:

$$\begin{aligned} V(\mathbf{Z},t) &= \frac{1}{2}[-a_{11}-b_{11}-1]Z_{\theta_1}^2+\frac{1}{2}\left[Z_{\theta_1}+Z_{\omega_1}\right]^2 \\ &\quad +\frac{1}{2}[-a_{22}-b_{22}-1]Z_{\theta_2}^2+\frac{1}{2}\left[Z_{\theta_2}+Z_{\omega_2}\right]^2+cZ_{\theta_1}Z_{\theta_2} \end{aligned} \tag{8}$$

where $c=\frac{1}{2}[a_{12}+a_{21}+b_{12}+b_{21}]$. If the Lyapunov candidate function (8) is positive definite function, then the coefficient $-a_{ii}-b_{ii}-1$ should be a positive value and the following inequality is derived.

$$G_{ii}\frac{\partial T_i}{\partial \theta_i}<-\frac{\partial H_i}{\partial \theta_i}, \qquad G_{ii}\frac{\partial T_i}{\partial \omega_i}<-\frac{\partial H_i}{\partial \omega_i}-1 \tag{9}$$
$$\Longrightarrow a_{ii}<0, \qquad b_{ii}+1<0$$

The right hand side terms originate from the term **H** (gravitational, Coriolis and centrifugal effects) which depends on state of musculoskeletal system. Since G_{ii} is always positive, $\frac{\partial T_i}{\partial \theta_i}$ and $\frac{\partial T_i}{\partial \omega_i}$ should take negative value which physically means the stiffness and viscosity of the joint. If these stiffness and viscosity can sufficiently suppress the right hand side terms, then, the term a_{ii} and b_{ii} are dominated by $\frac{\partial T_i}{\partial \theta_i}$ and $\frac{\partial T_i}{\partial \omega_i}$ respectively.

However, positive definiteness is not solely obtained by the condition (9). It can be easily shown by the following inequality induced by the inequality of arithmetic and geometric means.

$$\begin{aligned} V(\mathbf{Z},t) &\geq W(\mathbf{Z}) \\ &= N|Z_{\theta_1}||Z_{\theta_2}|+\frac{1}{2}\left[Z_{\theta_1}+Z_{\omega_1}\right]^2+\frac{1}{2}\left[Z_{\theta_2}+Z_{\omega_2}\right]^2 \end{aligned} \tag{10}$$

where $N=\min_t\left[\sqrt{a_{11}a_{22}}-\frac{|a_{12}+a_{21}|}{2}+\sqrt{(b_{11}+1)(b_{22}+1)}-\frac{|b_{12}+b_{21}|}{2}\right]$. $V(\mathbf{Z},t)$ is a positive definite function if the coefficient of $|Z_{\theta_1}||Z_{\theta_2}|$ is positive.

$$\sqrt{a_{11}a_{22}}-\frac{|a_{12}+a_{21}|}{2}>0,$$
$$\sqrt{(b_{11}+1)(b_{22}+1)}-\frac{|b_{12}+b_{21}|}{2}>0 \tag{11}$$

Substituting (7) to (11), the following inequalities are derived.

$$\gamma\geq\frac{[k_1+k_2]^2}{4k_1k_2}, \qquad \frac{[d_1+d_2]^2}{4d_1d_2} \tag{12}$$

where $\frac{\partial T_i}{\partial \theta_i}=k_i(t)$ is the stiffness of joint i, and $\frac{\partial T_i}{\partial \omega_i}=d_i(t)$ is the viscosity of joint i. As noted in (2), γ is determined by the geometric and mass distribution properties of the musculoskeletal system. Here, we define $\alpha(t)$ as the ratio between two joint stiffness values, and $\beta(t)$ as the ratio between two joint viscosity values.

$$\alpha(t)=\frac{k_i(t)}{k_j(t)}, \qquad \beta(t)=\frac{d_i(t)}{d_j(t)} \tag{13}$$

where $\alpha(t)$ and $\beta(t)$ are positive and less than 1. Then, (12) is rewritten by (13) as follows:

$$\gamma\geq\frac{[1+\alpha(t)]^2}{4\alpha(t)}, \qquad \frac{[1+\beta(t)]^2}{4\beta(t)}$$
$$\Longrightarrow 2\left(\gamma-\sqrt{\gamma^2-\gamma}\right)-1\leq 0.35\leq\alpha(t),\beta(t)\leq 1 \tag{14}$$

where the left hand side is calculated as 0.35 for $\gamma=1.30$. Condition (14) guarantees that (8) is a positive definite function if the values of the stiffness and viscosity between two joints are not considerably different. As a result, Lyapunov candidate function (8) can be a positive definite function if the condition (9) and (14) holds.

The next step is to investigate whether the total time derivative of the Lyapunov candidate function is negative definite or not. The total time derivative of the Lyapunov candidate function can be calculated as the following quadratic form:

$$\dot{V}(Z,t)=\mathbf{Z}^T\mathbf{P}(t)\mathbf{Z}<0$$

$$\mathbf{P}(t)=\begin{bmatrix} a_{11}-\frac{\dot{a}_{11}+\dot{b}_{11}}{2} & 0 & \frac{a_{12}+a_{21}}{2}+\frac{\dot{c}}{2} & \varepsilon \\ 0 & b_{11}+1 & -\varepsilon & \frac{b_{12}+b_{21}}{2} \\ \frac{a_{12}+a_{21}}{2}+\frac{\dot{c}}{2} & -\varepsilon & a_{22}-\frac{\dot{a}_{22}+\dot{b}_{22}}{2} & 0 \\ \varepsilon & \frac{b_{12}+b_{21}}{2} & 0 & b_{22}+1 \end{bmatrix} \tag{15}$$

where $\varepsilon=\frac{a_{12}-a_{21}+b_{12}-b_{21}}{4}\approx 0$ is negligible. As noted previously, error system (6) is asymptotically stable if

inequality is satisfied, i.e., $\mathbf{P}(t)$ is negative definite. The symmetric matrix $\mathbf{P}(t)$ is negative definite if the following conditions are satisfied:

$$G_{ii}\frac{\partial T_i}{\partial \theta_i} < -\frac{\partial H_i}{\partial \theta_i} - \delta_{ii}, \qquad G_{ii}\frac{\partial T_i}{\partial \omega_i} < -\frac{\partial H_i}{\partial \omega_i} - 1 \qquad (16)$$
$$\Rightarrow a_{ii} + \delta_{ii} < 0, \qquad b_{ii} + 1 < 0$$

$$\sqrt{(a_{11}+\delta_{11})(a_{22}+\delta_{22})} - \left|\frac{a_{12}+a_{21}}{2} + \delta_{12}\right| > 0, \qquad (17)$$
$$\sqrt{(b_{11}+1)(b_{22}+1)} - \left|\frac{b_{12}+b_{21}}{2}\right| > 0$$

where $\delta_{ii} = -\frac{\dot{a}_{ii}+\dot{b}_{ii}}{2}$, and $\delta_{ij} = \frac{\dot{c}}{2}$. Condition (16) have almost the same form as condition (9) except the existence of term δ_{ii} and δ_{ij}. Because δ_{ii} consists of the time partial derivative terms of $\dot{a}_{ii}$ and $\dot{b}_{ii}$, it physically represents how rapidly equilibrium point (target state) varies. Therefore, it is considered as an unstable term and requires that the negative stiffness $\frac{\partial T_i}{\partial \theta_i}$ of (16) takes on a more negative value than that of (9).

From the above Lyapunov stability analysis, we reach a conclusion that the most significant parameter to obtain self-stabilization is an actuator which can assign sufficient stiffness and viscosity in order to suppress unstable terms. The required minimum stiffness and viscosity which can guarantee self-stabilization depends on motion intensity and gravitational change. In this section, mathematical model to derive self-stabilizing condition of musculoskeletal system is solely used. In the next section, we use the physiological data of biological musculoskeletal system and investigate whether biological musculoskeletal system is designed to satisfy these mathematical conditions.

C. Biological Musculoskeletal System

In physiology and biomechanics, the negative gradient property of human joint torque with respect to joint angle and angular velocity is well known [13]. In the previous studies, Anderson [14] measured the maximum voluntary knee joint torque with respect to joint angle and angular velocity as shown in **Fig. 3**. Lee [15-17] also measured human ankle joint

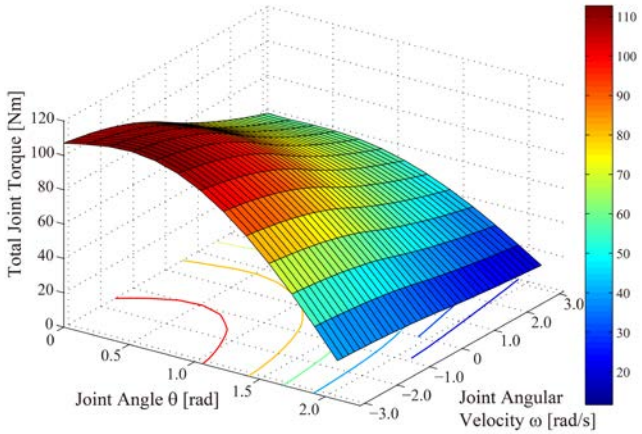

Fig. 3 Three-dimensional relationship among joint torque, angle and angular velocity of the human knee. Modified from [14].

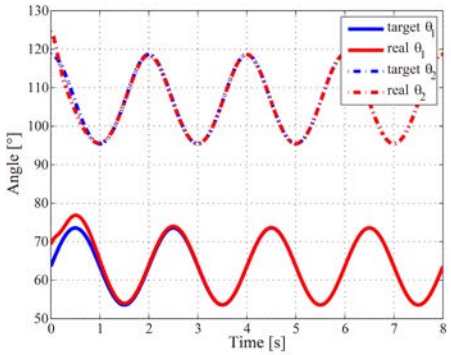

Fig. 4 The simulation results of time trajectories of the joint angle state of biological musculoskeletal system.

impedance with both relaxed and active muscles. The measured relaxed ankle stiffness is approximately 20 [Nm/rad] and this value increases to approximately 60 [Nm/rad] with 10% muscle activation. Based on these values, a simple mathematical Hill-type muscle model [18] is prepared for numerical simulation.

The numerical simulation results are shown as **Fig. 4**. As predicted by Lyapunov stability criteria (16), **Fig. 4** shows that red colored perturbed trajectories converge to blue colored target trajectories, which means that the origin of error system $\mathbf{Z}(t)$ is asymptotically stable. As a result, it is considered that biological musculoskeletal system has self-stabilizing function with its sufficient joint stiffness and viscosity.

III. Simulation and Experimental Results

Based on the results of the previous section, a self-stabilizing manipulator is designed in this study. The simulation and experimental results will be treated in this section. This manipulator moves in the vertical plane and has two revolute joints, which is the same as the model in **Fig. 2**.

A. Hardware Design Method

Fig. 5 (a) shows the manipulator designed for self-stabilization in this study. As discussed in the previous sections, the negative gradient properties of the joint torque are the most significant for the self-stabilization. And these negative gradient properties can be obtained by designing a new actuator. Two DC motors (Maxon EC motor, Switzerland) with a reducer (gear ratio of 6: 1), a variable radius gear transmission system (see **Fig. 5** (b)), and linear springs are implemented for the stiffness and viscosity of the joint.

The variable radius gear is a gear with a radius that is defined as a function of joint angle θ_i. This function is a monotonically decreasing function which means the gear ratio $\eta(\theta_i)$ monotonically decreases with respect to joint angle θ_i (i.e., $\frac{\partial \eta}{\partial \theta_i} < 0$ is always satisfied.). Joint torque T_i is expressed as (18).

$$T_i = \eta\zeta T_m - k_i\theta_i \qquad (18)$$

where T_m is the motor torque, $\eta(\theta_i)$ is the variable radius

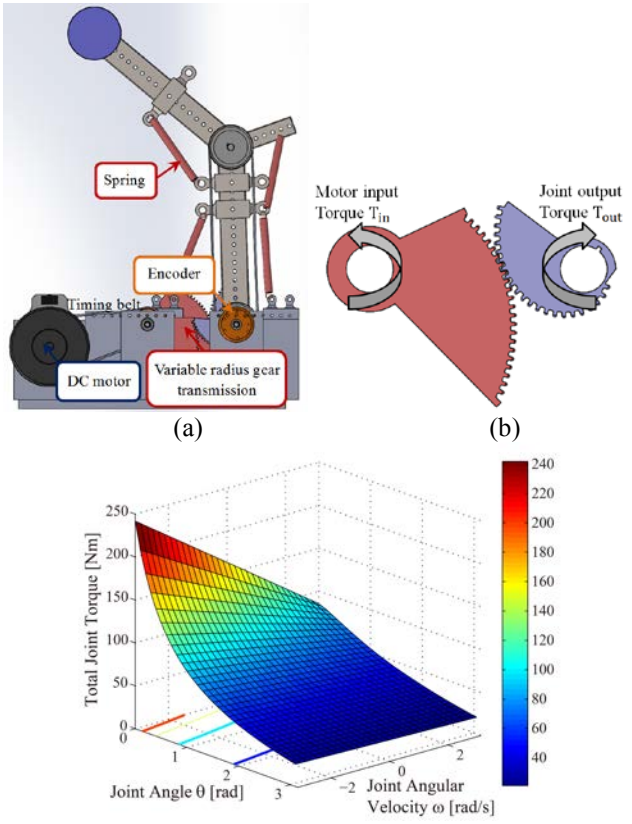

(a) (b) (c)

Fig. 5 Design of the self-stabilizing manipulator inspired by biological musculoskeletal systems. (a)Front view, (b) Variable radius gear transmission system for active stiffness, and (c) Three-dimensional relationship among joint torque, angle and angular velocity. $T_m = 4.570$ [Nm] case.

gear ratio, ζ is the constant gear ratio and k_i is the spring constant. Thus, the joint torque-angle gradient is calculated as follows:

$$\frac{\partial T_i}{\partial \theta_i} \simeq T_m \zeta \frac{\partial \eta}{\partial \theta_i} - k_i < 0 \qquad (19)$$

There are two kinds of stiffness in (19). One is passive stiffness $-k_i < 0$ induced by spring, the other is active stiffness induced by product of positive motor torque $T_m > 0$ and variable radius gear $\frac{\partial \eta}{\partial \theta_i} < 0$. Since this active stiffness is proportional to motor torque, it can provide additional stiffness for the self-stabilization. The torque-angular velocity gradient is calculated as follows:

$$\frac{\partial T_i}{\partial \omega_i} = \eta^2 \zeta^2 \frac{\partial T_m}{\partial \omega_m} < 0 \qquad (20)$$

where ω_m is the angular velocity of the DC motor. For the DC motor, the negative gradient property (i.e., $\frac{\partial T_m}{\partial \omega_m} < 0$) is always satisfied because of the back-electromotive force induced by the motor coil. As a result, **Fig. 5** (c) shows three-dimensional relationship among joint torque T_i, angle θ_i, and angular velocity ω_i. The negative gradient with respect to joint angle and angular velocity is identified.

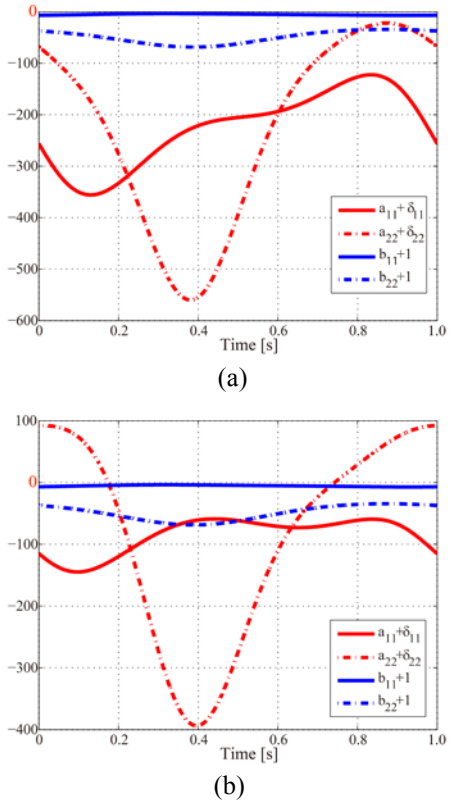

(a) (b)

Fig. 6 (a) Lyapunov stability criteria. Passive stiffness: 0.50 [kN/m] stable case, (b) Lyapunov stability criteria. Passive stiffness: 0.16 [kN/m] unstable case.

To determine the required stiffness and viscosity value of the joints for self-stabilization, the target motion should be determined first. Although the manipulator can be self-stabilized not only for periodic motion but also for any arbitrary motion, the target trajectory $\mathbf{X}_*(t)$ is selected as a 1.0 [Hz] periodic motion for demonstration in this paper. This target trajectory $\mathbf{X}_*(t)$ is described as an ellipse shape in the Cartesian coordinate as shown in **Fig. 1**. To satisfy Lyapunov stability criteria (16) with respect to the target motion, passive stiffness of spring is selected as 0.50 [kN/m]

Table I
Specifications of the self-stabilizing manipulator

Properties	Values	Unit
Length link 1 l_1	0.20	m
Length link 2 l_2	0.20	m
Mass M	0.30	kg
Mass link 1 m_1	0.23	kg
Mass link 2 m_2	0.23	kg
Stiffness of spring k_i	0.50 or 0.16	kN/m
Motor stall torque	4.570	Nm
Gear reducer ratio ζ	6	–
Viscosity of motor (with reducer)	0.72 (0.02×6^2)	Nms/rad

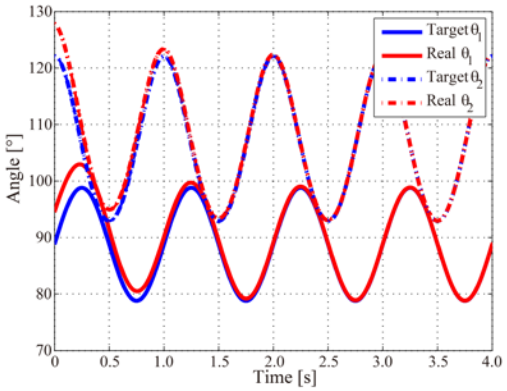

(a)

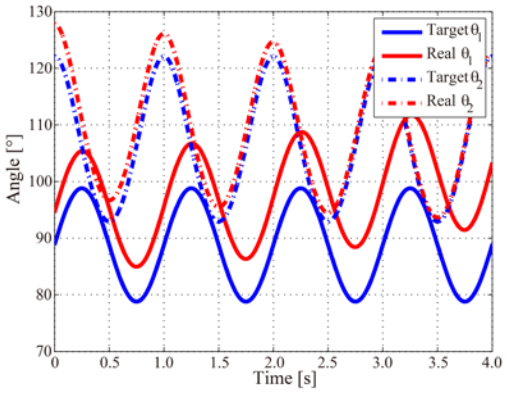

(b)

Fig. 7 Simulation results of time trajectory of joint angle. (a) Passive stiffness: 0.50 [kN/m] stable case. (b) Passive stiffness: 0.16 [kN/m] unstable case.

and viscosity of motor with reducer is selected as 0.72 [Nms/rad]. **Fig. 6** (a) shows that condition (16) is satisfied if these values are used. However, if the passive stiffness of spring decreases to 0.16 [kN/m], condition (16) is not satisfied as **Fig. 6** (b) shows. The specifications of the manipulator are as shown in **Table I**.

B. Simulation Results

Fig. 7 shows the simulation results. The stiffness of the spring is equally set to 0.50 [kN/m]. The red-colored curve is the perturbed trajectory $\mathbf{X}_*(t)$ and the blue-colored curve is the predicted target trajectory $\mathbf{X}_*(t)$. It is assumed that the initial error is occurred by disturbance at $t = 0$ [s]. As shown in **Fig. 7** (a), the initial error between the target and real trajectory decreases and approaches to $\mathbf{0}$.

However, if the stiffness of springs decrease to 0.16 [kN/m], the manipulator shows unstable motion as **Fig. 7** (b) shows. Condition (16) is a sufficient condition. Thus, it does not guarantee the instability of the system even if is not satisfied. However, **Fig. 7** (b) shows that the system in **Fig. 7** (b) is unstable when the sufficient condition (16) is not satisfied. Based on these results, the hardware experiment is implemented.

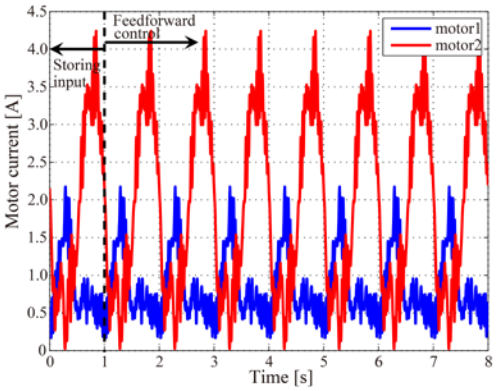

Fig. 8 Periodic control input for two DC motors.

C. Hardware Experimental Procedure

The block diagram of the open-loop control of the manipulator is shown in **Fig. 1** (b). Since there is no closed loop for external disturbance, the manipulator is controlled by an open-loop controller with previously defined motor input as shown in **Fig. 8**. To determine the open-loop control input for the DC motors, the searching control input process is prepared using the PD controller in this study. This PD controller automatically modifies control input in order to follow target trajectory and one period (i.e., 1.0 [s]) of this control input is stored for feedforward control.

After storing the control input, the manipulator is open-loop controlled with the stored control input and affected by external disturbances that cause angle and angular velocity error. The motor input does not change despite disturbances as shown in **Fig. 8**. In this paper, two cases of hardware experiment are treated. The one is the case that satisfies condition (16) with 0.50 [kN/m] springs, and the other is the case that does not satisfy condition (16) with 0.16 [kN/m] springs.

D. Hardware Experimental Results

Fig. 9 shows the hardware experimental results. **Fig. 9** (a) shows tha each joint angle of the red-colored trajectory converges to the blue-colored predicted target trajectory, after the external disturbance at $t = 4.0$ [s]. These results demonstrate that the manipulator has a self-stabilizing function because it satisfies condition (16).

However, as predicted in the simulation results of **Fig. 7** (b), this self-stabilizing function is lost as shown in **Fig. 9** (b) if the stiffness of the springs decreases to 0.16 [kN/m]. After extremely small disturbance at $t = 1.0$ [s], the error diverges with time and the manipulator collapses at the end. Since the case in **Fig. 9** (b) does not satisfy the sufficient condition, the self-stabilization is not guaranteed. These results imply that the sufficient condition for self-stabilization in (16) is less conservative sufficient condition.

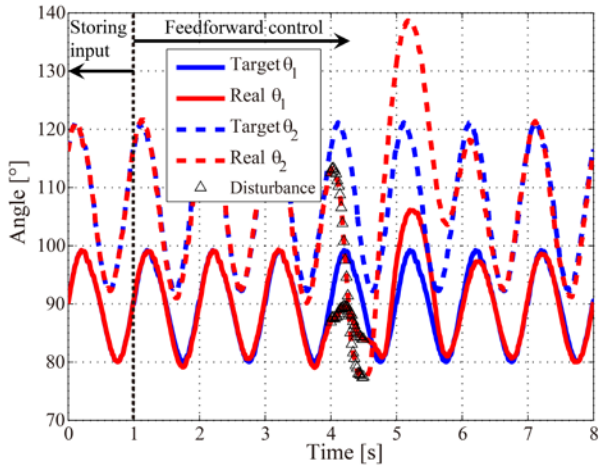

(a)

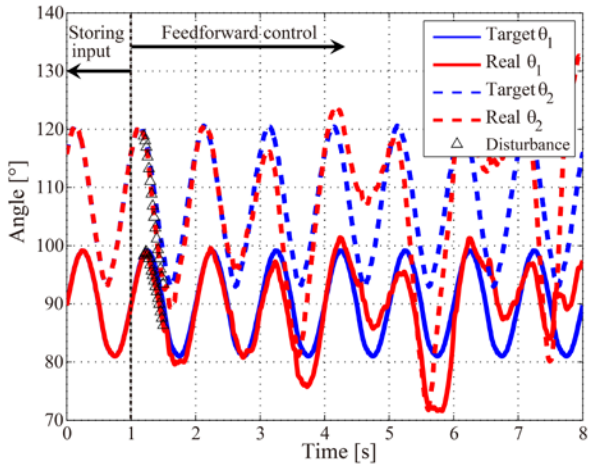

(b)

Fig. 9 Experimental results of time trajectory of joint angle. (a) Passive stiffness: 0.50 [kN/m] stable case. (b) Passive stiffness: 0.16 [kN/m] unstable case.

IV. Discussion

In general, the sufficient condition for stability is rather conservative. A large number of stability criteria for time-varying system often treat the fastest speed of varying eigenvalue as the unstable factor and the least negative eigenvalue as the stable factor. Thus, it tends to overestimate the unstable factor and underestimate the stable factor. As a result, it makes a condition for stability of time-varying system conservative. However, because the range of the stiffness of stable cases which does not satisfy the proposed self-stabilizing condition (16) is narrow, the sufficient condition proposed in this study is appropriate to design self-stabilized manipulators in engineering perspective.

As discussed in section II, condition (16) also treats the time derivative term δ_{ii} as an unstable term. This means that rapid change in motion (intensity of motion) requires much more stiffness of joints for self-stabilization. Thus, it is difficult to provide sufficient stiffness with respect to such a rapidly varying motion using a single type of spring stiffness. However, since both active stiffness mechanism and motion intensity are proportional to amplitude of motor torque, the self-stabilized manipulator in this study can correspond to wide range of motion intensity. It is well known that biological muscle also has the function that stiffness is proportional to muscle activation rate. Therefore, it is considered that active stiffness both the manipulator in this study and biological musculoskeletal system play significant role in maintaining self-stabilizing function.

The stiffness which is expressed as a negative gradient in angle-torque relation does not explicitly appear in the block diagram as shown in **Fig. 1** (a). However, since the state error induces the changes of joint torque through the DC motors and springs, the negative gradient works as a hidden feedback gain instead of PD controller. In view of control engineering, mathematically designed self-stabilizing function in this study plays the same role as both sensors and PD controller. This can explain why the manipulator in this study can be self-stabilized by open-loop control and it is considered that the stability of human motion depends on both self-stabilizing function of musculoskeletal system and feedback control of neural system. Since this kind of system that uses stabilizing dynamic properties of its body does not involve signal transmission and computation delay for feedback control, it does not become unstable in an environment where signal delays are considered.

V. Conclusion

In this study, the self-stabilizing function of a musculoskeletal system is analytically investigated using the Lyapunov stability theory. A Lyapunov candidate function is proposed and the sufficient condition for self-stabilization is obtained. The condition is the existence of negative gradient properties of torque with respect to joint angle and angular velocity.

From the numerical simulation results, it is considered that biological musculoskeletal system could have self-stabilizing function since its biomechanical data satisfies mathematically derived self-stabilizing condition in this study. From those results, a manipulator inspired by the self-stabilizing function of a musculoskeletal system is physically realized and the design method is introduced. Based on this condition, the negative gradient is realized by DC motors and springs and self-stabilizing function is identified in simulation and hardware experiment. Due to the implemented self-stabilizing function, the manipulator is stabilized from the external disturbances without any feedback control. If the manipulator does not satisfy the proposed condition in this study, stability of the manipulator is not guaranteed anymore.

Since this kind of self-stabilized manipulator does not require sensor based feedback control and heavy computation for control input, it is robust to signal delay. It is considered that the concept of self-stabilization is promising for stable motion control with open-loop control in robotics field.

REFERENCES

[1] Thorpe, Simon, Denis Fize, and Catherine Marlot. "Speed of processing in the human visual system." *nature* 381.6582 (1996): 520-522.

[2] Cordo, Paul, et al. "Proprioceptive coordination of movement sequences: role of velocity and position information." *Journal of neurophysiology* 71.5 (1994): 1848-1861.

[3] Kawato, Mitsuo, and Hiroaki Gomi. "A computational model of four regions of the cerebellum based on feedback-error learning." *Biological cybernetics* 68.2 (1992): 95-103.

[4] Bizzi, Emilio, et al. "Posture control and trajectory formation during arm movement." *The Journal of Neuroscience* 4.11 (1984): 2738-2744.

[5] Wagner, Heiko, and Reinhard Blickhan. "Stabilizing function of skeletal muscles: an analytical investigation." *Journal of Theoretical Biology* 199.2 (1999): 163-179.

[6] Wagner, Heiko, and Reinhard Blickhan. "Stabilizing function of antagonistic neuromusculoskeletal systems: an analytical investigation." *Biological cybernetics* 89.1 (2003): 71-79.

[7] Sugimoto, Yasuhiro, et al. "Stabilizing function of the musculoskeletal system for periodic motion." *Advanced Robotics* 23.5 (2009): 521-534.

[8] Chang, Handdeut, et al. "Self-stabilizing function of two dimensional human lower limb musculoskeletal system." *Robotics and Biomimetics (ROBIO), 2012 IEEE International Conference on*. IEEE, 2012.

[9] Plooij, Michiel, Wouter Wolfslag, and Martijn Wisse. "Open loop stable control in repetitive manipulation tasks." *Robotics and Automation (ICRA), 2014 IEEE International Conference on*. IEEE, 2014.

[10] Plooij, Michiel, et al. "Optimization of feedforward controllers to minimize sensitivity to model inaccuracies." *Intelligent Robots and Systems (IROS), 2013 IEEE/RSJ International Conference on*. IEEE, 2013.

[11] Vidyasagar, Mathukumalli. *Nonlinear systems analysis*. Vol. 42. Siam, 2002.

[12] Asada, Haruhiko, and Kamal Youcef-Toumi. *Direct-drive robots: theory and practice*. MIT press, 1987.

[13] Winter, David A. Biomechanics and motor control of human movement. John Wiley & Sons, 2009.

[14] Anderson, Dennis E., Michael L. Madigan, and Maury A. Nussbaum. "Maximum voluntary joint torque as a function of joint angle and angular velocity: model development and application to the lower limb." *Journal of biomechanics* 40.14 (2007): 3105-3113.

[15] Lee, Hyunglae, et al. "Multivariable static ankle mechanical impedance with relaxed muscles." *Journal of biomechanics* 44.10 (2011): 1901-1908.

[16] Lee, Hyunglae, et al. "Multivariable static ankle mechanical impedance with active muscles." *Neural Systems and Rehabilitation Engineering, IEEE Transactions on* 22.1 (2014): 44-52.

[17] Lee, Hyunglae, and Neville Hogan. "Investigation of human ankle mechanical impedance during locomotion using a wearable ankle robot." *Robotics and automation (ICRA), 2013 IEEE international conference on*. IEEE, 2013.

[18] Hill, A. V. "The heat of shortening and the dynamic constants of muscle." *Proceedings of the Royal Society of London B: Biological Sciences* 126.843 (1938): 136-195.